What is a spin glass? A glimpse via mesoscopic noise*

M. B. Weissman

Department of Physics, University of Illinois at Urbana-Champaign, Urbana, Illinois 61801-3080

It is an open question whether the slow dynamics of spin glasses is more accurately described by a model based on rather compact droplets which can flip thermally, or by a picture of more diffuse sets of flipping spins with properties described by hierarchical dynamics. Techniques have been developed for analyzing spontaneous fluctuations in mesoscopic samples which can directly address this question. In a well-known spin glass, *Cu*Mn, the experimental results are better fit by the hierarchical picture. Previously unexplored properties of the space of metastable configurations are directly measurable by these mesoscopic methods.

CONTENTS

I. INTRODUCTION

Spin glasses are often taken to be the most experimentally and theoretically accessible realization of systems with quenched (i.e., time-independent) disorder. Spin glasses differ from structural glasses in an important respect: the spin-glass Hamiltonian already contains random interactions, whereas randomness in a structural glass is quenched-in kinetically as the glass is formed. Thus it has been hoped that spin glasses would be easier to understand than ordinary glasses. Nevertheless, as the standard opening cliché goes, despite many years of intense effort, some of the most basic features of the spin-glass state (or states) remain obscure.[1]

A spin glass has a largely random-looking mixture of ferromagnetic and antiferromagnetic interactions. For example, in dilute solid solutions of magnetic atoms in nonmagnetic metals (such as *Cu*Mn, *Au*Fe, and many others of the best-studied classes of spin-glass materials), the spins interact via their oscillatory polarization of the conduction electrons (at half the Fermi wavelength, similar to Friedel oscillations). The random locations of the magnetic ions with respect to each other then give the random mixture of interaction signs.

It is, of course, impossible to satisfy simultaneously all the interactions in such a complicated jumble. Although systems with competing interactions are not necessarily complex, even without randomness it is often very hard to determine the ground state of large systems with such competing interactions. In fact, for spin glasses it remains an open question whether a unique or nearly unique ground state exists.

I shall take as the definition of a spin glass an empirical description of the phenomena that lead us to call a material a spin glass, rather than a formal Hamiltonian description. When the real part of the ac susceptibility of a material $[\chi'(\omega)\equiv\mathrm{Re}(\chi(\omega))]$ follows a roughly paramagnetic temperature dependence down to some temperature T_G, at which a sharp cusp occurs, the material is a candidate to be a spin glass. It is important that the deviations from paramagnetism of $\chi'(\omega)$ above T_G not be large enough for a ferromagnetic, ferrimagnetic, or antiferromagnetic transition to occur at T_G. Some (generally unidentified) degrees of freedom freeze at T_G (at least on the time scale $1/\omega$), but these involve spin-spin couplings with approximately random signs. The out-of-phase susceptibility $\chi''(\omega)\equiv\mathrm{Im}\chi(\omega)$ is essentially zero well above T_G, starting to rise just above T_G to a broad peak just below T_G (see Fig. 1). Notice that I have not specified the frequency ω; except for slight shifts of T_G, these phenomena are independent of ω for any ω well below a microscopic spin-relaxation rate. The typical range of $f\equiv\omega/2\pi$ in actual measurements is 10^{-3} Hz to 10^6 Hz. Thus the spin glass shares with ordinary glasses a broad range of characteristic relaxation rates below a rather sharply defined temperature.

The specific heat of spin glasses does not show any sharp feature at T_G or elsewhere, affording no easy identification with standard phase transitions. However, sharp features, apparently divergences at T_G, have been found in nonlinear susceptibilities, implying divergent correlation lengths for spin-spin correlation functions of order 4 and higher, such as the mean-square correlation

*The experimental work and much of the theoretical work described here was performed principally by N. E. Israeloff and G. B. Alers.

[1]See Binder and Young (1986), Dotsenko *et al.* (1990), and Fischer and Hertz (1991) for excellent reviews. When some reference seems called for but none is given, turn to these reviews. Many references to specific works relevant to the mesoscopic experiments may be found in Weissman *et al.* (1992), which also includes many experimental and theoretical details.

 0034-6861/93/65(3)/829(11)/$06.10

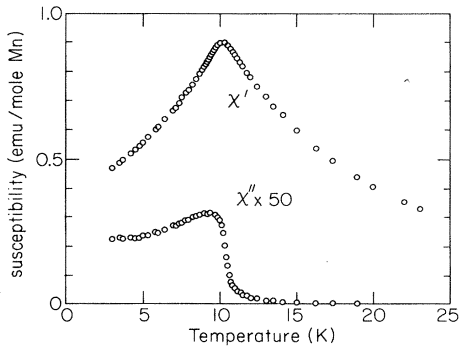

FIG. 1. The susceptibility components $\chi'(f,T)$ and $\chi''(f,T)$ shown for a typical spin glass, $Au_{1-x}Mn_x$ with $x \approx 0.03$ and $f \approx 200$ Hz (from Mulder *et al.*, 1981).

of spin pairs.

The materials that show spin-glass phenomena include not only metals with dilute magnetic solutes, but also some concentrated disordered magnetic metals (such as amorphous *Fe*Zr) and partially disordered magnetic insulators (such as $Eu_xSr_{1-x}S$). (In some cases the spin-glass state forms as a ferromagnetic state is further cooled, requiring some modification of our definition). Although in all cases both randomness and complicated competing interactions are present, the extent to which these different materials have similar spin-glass order is not known.

I plan first to introduce qualitatively some diverse spin-glass models, including the well-known droplet model and models of hierarchical kinetics. Then I shall discuss the simplest mesoscopic predictions of droplet and hierarchical models. With the introduction of the measurement technique and initial results, we shall see that the simplest droplet pictures are inapplicable. Then some new higher-order scaling techniques will be introduced to distinguish between more complicated droplet pictures and generic hierarchical pictures. Finally, being unable to describe the results in a droplet picture, I shall give some of their implications in a hierarchical framework. Along the way some extra bits of information, such as dynamical coherence sizes, will emerge.

II. THEORETICAL MODELS

There have been many theoretical approaches to describing spin-glass states. I shall not attempt here to describe them completely, but shall introduce several that give a feel for the range of these theories. Two pictures—the droplet theory and a picture of hierarchical kinetics—will be presented in just enough detail to provide motivation for the experiments reported in Sec. IV.

The earliest theory for anomalous properties of dilute magnetic atoms in transition metals is due to Overhauser (1959). He proposed that the host metal forms a spin-density wave (SDW) with a q vector whose magnitude is determined by the conduction-electron Fermi surface. The magnetic atoms align with the SDW, providing the negative free energy required for thermodynamic stability. It is unclear in several recent descriptions of this model whether the ground state would be a single SDW with which each local moment aligns or if the random placements of the local moments would favor breakup into SDW domains to increase the resulting polarization at the magnetic atoms (Mydosh, 1988; Werner, 1990). Oddly enough, although this theory has fallen into disfavor, it is the only one supported by direct evidence, in that neutron scattering on *Cu*Mn and *Ag*Mn shows the presence of a set of SDW-like components with wave vectors incommensurate with the lattice and with coherence lengths of roughly 4 nm (Mydosh, 1988; Werner, 1990). We shall see that mesoscopic experiments on a 50-nm scale reinforce the strong impression given by finite-size-effect measurements (Sandlund *et al.*, 1989; Gavrin *et al.*, 1990) that this coherence length is much shorter than the spin-glass dynamical correlation lengths.

Feigel'man and Ioffe (1984) predicted that a "hierarchical superparamagnet" with spin-glass-like properties should form if each spin interacts with a large number of its neighbors, as one would expect for interactions via incipient SDW's. Whether the hierarchical kinetics to be described below has anything to do with the hierarchical superparamagnet is beyond my current understanding.

A highly accessible picture, known as droplet scaling, explicitly focuses on spatial correlations among spins as the key to understanding the slow dynamics, as well as the critical behavior, of spin glasses (Bray and Moore, 1987; Fisher and Huse, 1988a,1988b). In this picture, the ground state is unique except for any obvious symmetries of the Hamiltonian, as is any pure state at any low temperature. Because spin-coupling terms in the Hamiltonian are random, the typical energy required to turn over any compact blob of spins does not scale as its surface area (as in a conventional ordered phase) but as some lower power of the linear dimension L. One might at first guess that, since the interactions between spins have random sign, this interaction energy would scale as the square root of the surface area. However, since the lowest-energy surface of a thermally flipped blob will not be a randomly picked surface but rather one that minimizes the energy cost of flipping the blob, the actual scaling exponent turns out to be lower than this simple guess. More importantly, this typical energy scale only sets the width of a distribution of energies which goes smoothly to a finite density at zero splitting. Therefore, the probability of finding large blobs that can turn over at a cost of less than about kT (at finite temperature) goes to zero only as a power of L. There is not an exponential freezing-out of finite-size droplets, such as would be found for nonrandom interactions.

If one adds the plausible assumption that the Arrhenius activation energy, i.e., the energy barrier determining the rates of the droplet flips, also shows scaling in L, one obtains a wide spectrum of relaxation times. The

essence of the droplet explanation for this spectrum is that slow events come from big droplets, while fast events come from small ones.

The droplet approach relies crucially on the finite range of the interaction and on the presumed spatial scaling of the characteristic energies. An opposite approach (Sherrington and Kirkpatrick, 1975) is to simplify the Hamiltonian by completely ignoring all spatial properties, letting every pair of spins interact with equal probability. That simplification, of course, raises the distinct possibility that the solution will miss important real-space correlations in the actual states. With this simplification, the spin-glass problem has actually been formally solved (at least within certain approximations) by Parisi and co-workers, as described previously in this journal (Binder and Young, 1986) and elsewhere (Mézard *et al.*, 1987).

The most striking feature of the Parisi solution is that infinitely many states, unrelated by any simple symmetries, are found for an infinite system. ("State" here is meant in the sense of a pure thermodynamic state—a set of configurations in thermal equilibrium with each other.) Since any two distinct states differ by an infinite number of spins, the time required to convert from one to the other is infinite, just as the time required for a ferromagnet to flip spontaneously from spin-up to spin-down is infinite. It is the fluctuations within an individual state among long-lived configurations, differing by a large but not infinite number of spins, that give measurable slow dynamics. [So far, approximate theoretical attempts to analyze these intrastate dynamics in the Parisi theory indicate that their spin-fluctuation spectrum should be closer to $\omega^{-1/2}$ than to ω^{-1}, in contradiction to all experimental data (Sompolinsky and Zippelius, 1982)]. Therefore any connection between the unusual space of states and the observed dynamics can only be indirect.

Such an indirect connection has been proposed on the basis of a guess that a very special topology found for the Parisi-state space might also apply to the space of long-lived spin configurations within any particular state. The topology of the set of states can be described using a simple metric based on the "Hamming distance" D (Rammal *et al.*, 1986). D is simply the fraction of spins that must reorient to convert one state to another. Surprisingly, with this metric the distances between low-lying states in the Parisi picture can be represented by a tree on which the states are the end points, as in Fig. 2. The distance between any two such points is represented by the height to which one must go on the tree to connect those points. Spaces on which the metric has such a representation are called ultrametric (Rammal *et al.*, 1986). This ultrametric topology is a special property, absent in generic metric spaces. A similar metric, proportional to the (finite) number of spins that must flip to convert one configuration to another, may be used on configuration space, but the resulting topology is unknown.

The ultrametric structure of the Parisi-state space has led some theorists (e.g., Ogielski and Stein, 1985; Paladin *et al.*, 1985; Schreckenberg, 1985; Bachas and Huberman, 1986; Maritan and Stella, 1986; Sibani, 1987) to wonder about what sort of dynamics might be observed in spaces with hierarchical (i.e., ultrametric) structure. Again, such hierarchical kinetic pictures would describe dynamics among metastable configurations, not among the pure states described by Parisi. Such hierarchical kinetic descriptions can also be motivated by pictures other than the Parisi solution. As Ogielski and Stein point out, a variety of systems describable by rough energy landscapes might show hierarchical kinetics, with higher vertices corresponding to higher barriers.

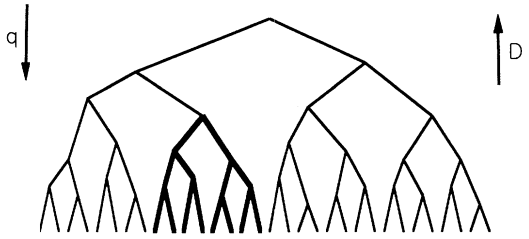

FIG. 2. A bifurcating hierarchical tree. The actual spin states are represented by the end points of the lowest branches. The Hamming distance D between any two states is represented by the height of the highest vertex in the lowest path connecting the states. The state overlap q is greatest between states with the least D. The barrier height between any two states is presumed to be a finite monotonic increasing function of D. Thus on the time scale of a given experiment only part of the hierarchy, e.g., that shown in thick lines, will be explored. Bifurcations are shown only for simplicity.

The central point of this paper is that the dynamics on ultrametric spaces has characteristic measurable signatures distinct from the dynamics of, for example, collections of droplets. The trick is to find the right dynamical properties to measure.

In order to make a sensible, simple kinetic theory, one assigns to each vertex on the tree some characteristic time τ for transitions between the clusters of states descending from that vertex. Vertices connecting distant clusters, i.e., high-D vertices, should correspond to long times.

Theorists have explored a variety of plausible monotonic maps from D to τ. The simplest such map assigns to each tree vertex an Arrhenius barrier height proportional to D. The typical value for D between the starting and final state then grows logarithmically with time, $D(\tau) \propto \ln(\tau)$. Ogielski and Stein, in particular, calculated both $D(\tau)$ and how the probability $P(\tau)$ of being in the initial state (or branch) would decrease as a function of time. We shall see that both $D(\tau)$ and $P(\tau)$ are measurable in mesoscopic experiments. (The reader should beware the occasional reference that casually assumes that these two functions are closely related.)

A word of caution is in order. If the mesoscopic spin-glass dynamics turns out to show the properties of a kinetic hierarchy, we shall not be justified in assuming a simple map from that hierarchy to the Parisi-state space which loosely inspired the hierarchical picture. Certainly, if we are to speak of the fraction D of spins that reorient in some event, we must mean the fraction of some finite set. Further hypotheses, such as the existence of some large but finite volumes within which long-lived configurations show hierarchical kinetics, might be required.[2]

Both the droplet picture and the hierarchical kinetics picture predict a broad range of characteristic relaxation rates. The precise form of the distribution in the droplet picture depends on some scaling exponents, as well as on any deviations from asymptotic scaling that real materials with nonrandom distributions of interactions might show. For hierarchical pictures, the form of the distribution depends on several factors, including the poorly understood map from D to τ. Within the theoretical error bars, since neither picture is meant to be taken unduly literally, both predict $\chi''(\omega)$ independent of ω over a wide range or, equivalently, that the frequency spectrum of fluctuations in the magnetic moment, $S_M(f)$, is $\propto 1/f$. For both types of theory, that form arises simply because τ depends exponentially on the barrier height, and these barriers have a reasonably broad distribution (Weissman, 1988). Thus conventional measures of linear-response functions or of fluctuation spectra are poorly suited for answering the qualitative question of which approach is more suitable.

As a result, it has been possible for experimenters simply to choose which type of approach should be used to design experiments or interpret data. Roughly speaking, the Parisi approach has been followed in continental Europe and the droplet approach in English-speaking countries. So long as the models remain pictured in entirely different spaces, and their followers remain separated by at least a channel, there seems little danger of either approach failing an awkward experimental test.

For anyone perversely tempted to challenge this comfortable arrangement, the two obvious experimental avenues for discriminating between the theories would be to find creative uses of nonlinear perturbation experiments or of higher moment non-Gaussian statistics of fluctuation experiments. The Saclay and UCLA groups have shown that combined temperature-field perturbation experiments have a natural interpretation in terms of a hierarchical picture (e.g., Lederman *et al.*, 1991). However, in part because the droplet scaling picture has been shown (e.g., Bray and Moore, 1987) to imply that equilibrium spin-spin correlation functions change chaotically as a function of temperature for distant spins, it has been difficult to calculate just what the droplet picture predicts for such experiments. (David Huse tells me that similar complications are present for the infinite-range model.)

III. QUALITATIVE FEATURES OF MESOSCOPIC FLUCTUATIONS

Having spent some time working out statistical analyses of $1/f$ noise in mesoscopic systems to show how non-Gaussian statistics can distinguish between different kinetic models that give identical spectra, it was natural for my group to look at the possibility of examining the fundamental pattern of spin-glass dynamics via noise techniques (Weissman, 1988). Here, by "mesoscopic," I do not mean anything about quantum coherence lengths, just that a sample is small enough for non-Gaussian statistical effects to be measured but large enough for the physical effects to resemble those of bulk samples.

The central expectation for the simplest Ising droplet picture, in which the droplets form noninteracting two-state systems, is that in a given mesoscopic sample at a given temperature only a finite set of droplets will be present. Fluctuation spectra (e.g., of the magnetization), like those of other collections of noninteracting two-state systems, would then consist of the superposition of discrete components, each with a characteristic frequency, ω_i, corresponding to the relaxation rate of an individual two-state system. In the simplest case each component is a Lorentzian, $\omega_i/(\omega^2+\omega_i^2)$. Large deviations from a $1/f$ spectrum would then be apparent, accompanied by slightly non-Gaussian fluctuation statistics (Weissman, 1988).

Qualitatively, a hierarchical picture would give very different fluctuation statistics. At a given time the spin glass would be in some state represented by an end point of the tree. If many successive measurements are made, the spin glass will be found to fluctuate back and forth between several states connected by vertices whose height is determined by the characteristic time scale of the measurements. For example, the system might fluctuate among the eight states represented by the darkened portion of the tree in Fig. 2. There are seven vertices in that part of the tree, representing seven different relaxation rates—as expected for a system that must be in one of eight states. Thus for a while a set of characteristic rates, not especially different from those that might be found for a collection of droplets, should appear in the spectrum.

If the same measurement is made repeatedly, the system will have a chance to leave the initially accessible region of the tree by slow transitions over higher vertices. The fine structure of these newly accessible branches, which gives the detailed fluctuation spectrum in the analysis range, will have nothing in common with the original branches. The old set of relaxation rates and

[2]In the experiments to be described, the use of mesoscopic samples provides a natural excuse for letting the number of coherent spins be finite. However, this excuse should not be seized upon too readily, since there is no indication that the average dynamics in mesoscopic and macroscopic samples is much different.

amplitudes will be replaced by a new set. Thus the spectral shape will wander in time, giving significantly non-Gaussian fluctuation statistics.

If spectral wandering is found, however, one cannot rule out the possibility that *interacting* droplets are present. A droplet whose characteristic rate falls within the observed spectral range may occasionally be created or destroyed, or have less drastic modifications of its effective Hamiltonian, by the flipping of a larger droplet that is nearby or even overlapping. Thus interacting droplets can produce spectra that change in time. The distinction between hierarchical pictures and interacting-droplet pictures will be described later.

Thus I believed that mesoscopic fluctuation experiments could in principle distinguish between simple droplet-like kinetics and hierarchical kinetics. Because of the dubious relevance of the assumptions leading to the hierarchical kinetics picture, and because of my personal lack of understanding of the derivation of the ultrametricity of the Parisi solution, I approached the mesoscopic fluctuation experiments with a bias in favor of a droplet interpretation. However, I was somewhat pessimistic as to whether in a realistic case of interacting droplets we could unambiguously rule out hierarchical interpretations. Experiments on *Cu*Mn required the modification of my expectations that the droplet picture would basically work and that the results would be uncomfortably ambiguous.

Although magnetization is the obvious variable to measure in a spin-glass-fluctuation experiment (Ocio *et al.*, 1986; Reim *et al.*, 1986), the current generation of SQUID detectors did not seem to be quite sensitive enough to allow mesoscopic measurements of spin-glass noise. Thus some suitable mesoscopic probe was needed. Inspired by the SDW picture of the spin-glass state in *Cu*Mn and an analogy to resistivity noise in the SDW of Cr, we (meaning Nate Israeloff, with me as a discouraging bystander) measured resistivity fluctuations in *Cu*Mn. To my surprise, the spin fluctuations were the principal source of $1/f$ noise in the spin-glass regime. However, unlike the magnetization noise, the resistivity noise continued to grow as the samples were cooled below their respective T_G's, as shown in Fig. 3 (Israeloff *et al.*, 1989).

The explanation of the large low-T noise lay in a previously published theory (Al'tshuler and Spivak, 1985; Feng *et al.*, 1987). Since the Mn spins affect the potential seen by the conduction electrons, interference terms in the static spin scattering make the conductivity sensitive to the relative orientation of the Mn spins. The approximate magnitude of the relevant scattering term may be inferred from T_G, since this same effect on the conduction electrons leads to the principal spin-spin coupling in *Cu*Mn and related materials. The most important interference terms are the multiple-scattering effects that give rise to the "universal" conductance fluctuations (UCF's). These grow at low temperature as the inelastic-scattering time grows and the thermal smearing of the Fermi level is reduced. Thus the noise magnitude

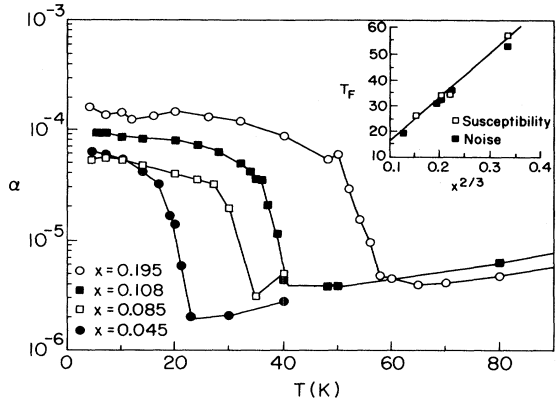

FIG. 3. Values of $\alpha(T)$, a dimensionless measure of the size of the resistance noise (Weissman, 1988), shown for several concentrations, x, of $Cu_{1-x}Mn_x$ in macroscopic samples. The inset shows that the magnetic transition temperatures and the noise-increase temperatures closely track each other as a function of x.

can and does increase at low temperature even as the number of fluctuating units (spins in this case, structural defects in others) decreases. The UCF theory, although rough in spots, predicted the absolute magnitude of the noise to within about a factor of 3 and also approximately gave its temperature dependence (Israeloff *et al.*, 1989). Any SDW-like anisotropy in the resistivity tensor turned out to be too small to matter. More recent experiments have directly shown that frozen spin configurations can give UCF magneto-fingerprints (de Vegvar *et al.*, 1991).

The sample size needed to observe mesoscopic effects can be guessed *a priori*. Finite-size-effect measurements (Sandlund *et al.*, 1989; Gavrin *et al.*, 1990) show that T_G is substantially lowered by reducing any of the sample dimensions much below 50 nm, so it is hard to call smaller samples mesoscopic in the sense defined above. From the linear specific heat, we know that at temperatures up to T_G the density of states of elementary excitations cannot be so large as to make the noise statistics Gaussian in samples with dimensions of the order of 15 nm. Our first samples had dimensions of roughly 50 nm × 50 nm × 150 nm, which proved adequate.[3] These samples contained roughly 10^8 atoms in the bridge, or about 10^7 spins, since the Mn concentration was 9 at. %.

[3]Glen Garfunkel developed a two-dimensional step-edge technique, which he calls "a poor man's nanolithography," for making small enough samples via optical lithography (Garfunkel and Weissman, 1990). Israeloff further modified the technique so that the nanobridges between macroscopic pads could be made after ordinary deposition on a flat substrate. This modification is useful for any film, but particularly useful in other experiments in which, for example, mesoscopic bridges in epitaxial films are desired. Other experimental techniques are described in our more technical papers (Israeloff *et al.*, 1991; Alers *et al.*, 1992; Weissman *et al.*, 1992).

The mesoscopic samples show noise spectra similar to those of larger samples, although their T_G is a bit lower than in bulk, presumably an effect of increased surface area. Averaged over enough time and over several cooldowns, the resistance noise spectra, $S(f)$, were still of the form $f^{-\gamma}$, with $\gamma=1.00$. The noise intensity increased to about the same level in the mesoscopic samples as in the larger samples (with a conventional volume normalization, see Weissman, 1988). Above T_G the mesoscopic samples were somewhat noisier. Glenn Alers showed that on rapidly cycling the temperature to above T_G and back, the resistance R changed by a random amount close to the UCF prediction, confirming sketchy earlier results.

Some of the initial noise spectra are shown in Fig. 4. Each spectrum is obtained from 40 min of data. They are taken consecutively, with no change of conditions during or between spectra. The dramatic differences between different spectra are not a result of a monotonic drift, such as that found in macroscopic aging effects. (Alers found a small systematic drift by averaging several data sets, but it becomes lost in the random wandering after a few hundred seconds.)

At this point, without any fancy analysis and without any ambiguity, we can flatly state that the *Cu*Mn spin glass in the experimental regime cannot be described by a noninteracting-droplet model. The spectrum wanders, rather than settling into a sum of fixed components from the different droplets. Qualitatively, this spectral wandering is similar to our prior expectations for hierarchical kinetics. More than qualitative impressions are needed, however, to decide whether the details of the noise statistics are better described by a truly hierarchical model or by a model of interacting droplets.

Before entering into that tricky question, it helps to view some traces (Fig. 5) of $\delta R(t)$, which show some clearly identifiable discrete events. The UCF theory provides a way of calculating about how many spins coherently flipping are likely to be required to produce an event of this size. That number is about 10^4 for the events illustrated. A more sophisticated analysis uses the net size of the non-Gaussian spectral wandering, which is inversely proportional to the density of independent sets of spins contributing to the spin dynamics in a given frequency range. The known χ'' gives the density of spins contributing to the dynamics in that same range. Together, these numbers give a value for the number of spins per coherently flipping set, slightly larger than 10^4. That these large numbers of spins act as a unit is not too surprising within either a droplet picture or a hierarchical one, but does confirm the presence of coherent units much larger than the apparent SDW domains. An additional implication is that the total entropy associated with all the slow modes (i.e., those in the $1/f$ regime, up to about 10^9 Hz) is much less than one per spin. Thus the low-temperature specific heat does not reflect these slowly fluctuating modes, in sharp contrast to the situation in structural glasses.

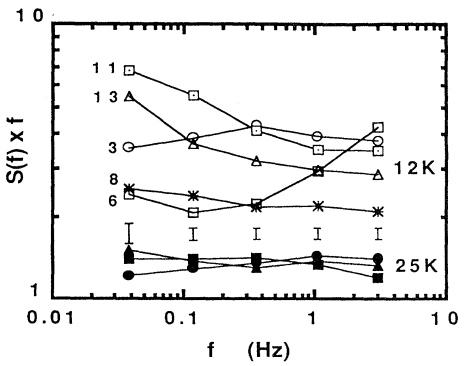

FIG. 4. Measurements of the resistance noise spectrum at $T=25$ K and at about 12 K for a $Cu_{0.91}Mn_{0.09}$ sample containing about 2×10^6 spins with $T_G\approx24$ K. Each spectrum is a 40-minute average derived from 100 Fourier transforms. A $1/f$ spectrum appears as a horizontal line in this representation. The set of error bars shows the calculated Gaussian standard deviation. The 12-K spectra are labeled by the order in which they were taken, with many omitted to avoid clutter.

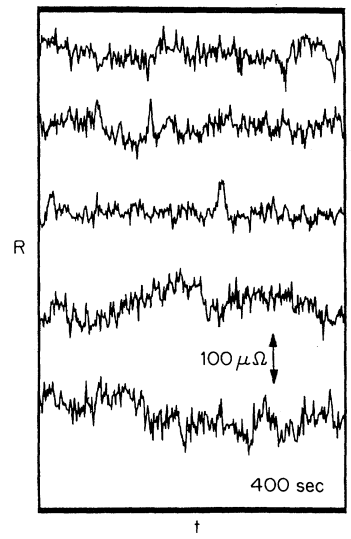

FIG. 5. Records of $\delta R(t)$ from a sample containing about 6×10^6 spins taken at 17 K. A few well-defined events can be discerned.

The $\delta R(t)$ traces also show something surprising. When switching between discrete resistance levels can be identified, we observe that it does not usually repeat many times, although about 100 switches occurred once before the switching ceased. This behavior contradicts expectations for two-state droplets (even ones with some degree of interaction) and also seems surprising for a simple bifurcating hierarchical tree, for which any vertex in the ascending tree from the current state represents a mode of switching between two clusters of states. Leaving the region of the tree which descends from some vertex requires a transition over a higher vertex, which should not happen too frequently. We shall return to this point.

IV. STATISTICAL ANALYSIS OF MESOSCOPIC FLUCTUATIONS

The simplest droplet picture, in which the droplets would be noninteracting two-state systems, makes definite predictions that are flatly contradicted by the data. Hierarchical models also make specific predictions, one of which we had figured out prior to the experiments. The measured variable (magnetization or conductance) is not completely randomized by configuration changes with small D. In fact, the mean squared difference in R between any two states should grow linearly with their D up to some saturation point. The fine structure of a tree branch, however, has, so far as anyone knows, no reason to have any more in common with a nearby branch than with a distant one. Even minor changes in barrier heights are enough to make a spectrum look entirely different. Therefore the memory function which describes how the resistance or magnetization forgets its initial random value has a long-time tail longer than the memory function describing how the detailed shape of the fluctuation spectrum forgets its initial random value. This difference is explicitly calculated for some models by Ogielski and Stein (1985).

We thus need quantitative measures of the spectral wandering. These can be provided by a set of measures that we call the second spectra, obtained as follows. The resistance noise spectrum $S(f)$ in Fig. 4 is not measured by an ideal ensemble average but rather by taking discrete data points (usually sets of 1024), Fourier-transforming, and squaring them to obtain 512 discrete spectral points. (The number of variables is reduced by half in squaring the complex transform.) Since any one of the resulting spectral points has a large uncertainty, due to effects of sampling any random signal, and since $1/f$ noise has no interesting structure on scales less than about an octave (Weissman, 1988), we then sum these points by octaves (of which at most nine are usable). This procedure reduces the set of numbers with which we must deal and also reduces their fractional uncertainty. Now a new set of 1024 data points may be taken and reduced to nine new octave sums. The entire procedure can be repeated to obtain a large (e.g., 1024 points) time series of sets of octave sums.

Given a time series, the obvious thing to do is to Fourier-transform and square it (obvious, at least, to anyone who does that for a living). The square of the Fourier transform of the time series of octave sums taken in an octave around f, normalized by the square of the mean value of that series, gives the second spectrum $S_2(f_2,f)$. That is,

$$S_2(f_2,f)=\langle |F(O(f,t))|^2\rangle / \langle O(f,t)\rangle^2 ,$$

where $O(f,t)$ is the integral of $S(f)$ over an octave around f taken from data measured near time t, and F is the Fourier operator. An integral of $S_2(f_2,f)$ over f_2 (e.g., a second octave sum) is a dimensionless number, since it is a fourth moment divided by the square of a second moment of the variable.

It helps to remember that $S_2(f_2,f)$ is the Fourier transform of the autocorrelation function of the time series of the noise power in an octave around f, $\langle O(f,t)O(f,t+\tau)\rangle$. Thus, at least for small f_2, the dependence of $S_2(f_2,f)$ on f_2 is simply obtained by Fourier-transforming the memory function describing the long-time persistence of features in $S(f)$.

Physically, this second spectrum is just a (conveniently normalized) spectrum of the wandering of the ordinary noise power near f. The size of $S_2(f_2,f)$ tells us something about how much wandering there is, while its dependence on f_2 tells us how the memory of the spectral shape decays in time. In a hierarchical scheme, for example, this combination provides information about the density (versus log time) of vertices (see Fig. 2 again) and about whether the entire sample acts as a single hierarchy. In a droplet interpretation, $S_2(f_2,f)$ provides information on the density of droplets within the interaction range of any particular droplet.

One can also obtain the normalized cross spectra between two different octave-sum time series, centered on frequencies f_a and f_b, which we denote $S_2(f_2,f_a,f_b)$. For equilibrium systems, only the real part of such cross second spectra has a nonzero expectation value; but for driven dynamical systems, its imaginary part should provide information on energy flow between different frequency scales.

These cross second spectra tell us whether, in the slow wandering of the spectral shape, the noise powers near f_a and f_b wander together or independently. That information, in turn, can tell us whether the individual units that temporarily contribute to the ordinary spectrum do so through Lorentzians (like simple two-state systems) or through broader spectra (like those of multistate systems).

Now we can restate our prior predictions and work out some new ones in terms of S_2. For noninteracting two-state systems, $S_2(f_2,f)$ is white, i.e., independent of f_2 (Weissman, 1988). For generic hierarchical pictures, $S_2(f_2,f)$ has a low-frequency slope reflecting the long-time tail of the probability of returning to the initial branch. Returning to our starting point about the difference between that memory function and $D(\tau)$ for hierarchical kinetics, but now in Fourier space, we now expect the slope $-\partial \ln[S_2(f_2,f)]/\partial \ln f_2$ to be smaller than $-\partial \ln S(f)/\partial \ln f$. In a simple Ogielski-Stein model, the likelihood of being in the initial state asymptotically decays as $\tau^{-\beta}$, where β is proportional to the density of vertices on each branch and inversely proportional to temperature; thus $S_2(f_2,f)$ should be proportional to $f_2^{-(1-\beta)}$.

We can immediately check some of the second spectra (Figs. 6 and 7). They are, of course, not white, as was immediately apparent when we found $S(f)$ to wander slowly. They all also turn out to be slightly flatter than $1/f$ (which appears horizontal on these plots); their degree of flattening, β, grows with T, as one would guess from very

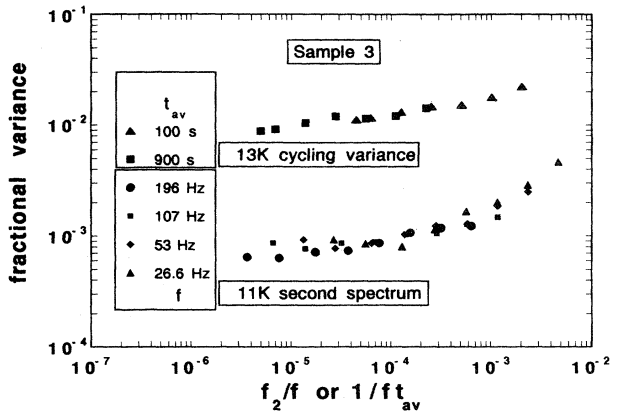

FIG. 6. The ratio $\langle(\delta S_1(f))^2\rangle/\langle S_1(f)\rangle^2$, nearly scale invariant, i.e., independent of f for fixed $ft_{\rm AV}$ or fixed f/f_2 ($t_{\rm AV}$ is the averaging time for a given data set). Top: $\langle(\delta S_1(f))^2\rangle/\langle S_1(f)\rangle^2$ from each of seven different octave bands of $S_1(f)$, measured at 13 K (with $T_G\approx 28$ K) by comparing spectra taken after 12 thermal cycles above T_G. Different groupings of the same data give $t_{\rm AV}=900$ sec and $t_{\rm AV}=100$ sec. Bottom: $S_2(f_2,f)$ at 11 K obtained as cross spectra between power fluctuations in adjacent octaves (to nearly eliminate Gaussian effects), plotted as $\langle(\delta S_1(f))^2\rangle/\langle S_1(f)\rangle^2$ per octave of f_2.

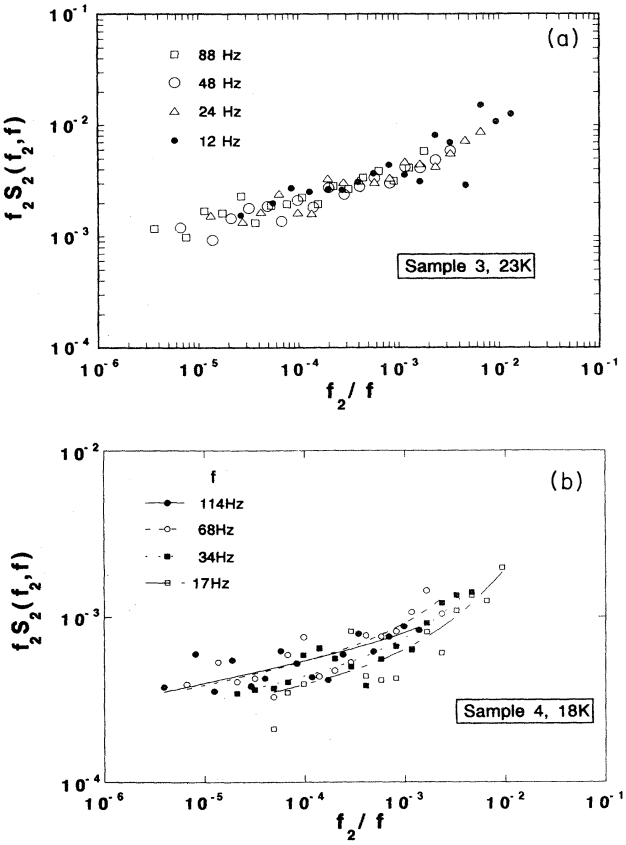

FIG. 7. Second spectrum illustrated in scale-invariant form for two samples.

simplified models. Hierarchical pictures thus have at least a chance to describe the data.

We now turn to a different type of scaling: the dependence on f of $S_2(f_2,f)$ and of other mesoscopic effects. Remember that a central point in extracting dynamics from the droplet picture was the idea that big droplets are slower than fast ones. The lower-frequency noise then comes from a smaller number of larger elements, while the higher-frequency noise comes from a larger number of smaller elements.

One way to determine the density of independent fluctuating units per octave is to compare noise spectra taken over a complete ensemble. The greater the density of fluctuating elements, the smaller the deviations from the ensemble average. This ensemble variance can be obtained by comparing spectra taken below T_G after successive cycles to above T_G. (In an equilibrium droplet picture, one would expect to obtain the same detailed spectrum on each cycle, but droplets stuck in metastable minima might give something like the same variability expected for hierarchical pictures.) On first inspection, the fractional variance in $S(f)$ over the ensemble seemed to be a decreasing function of f, so that a finite scaling exponent relating droplet size to barrier height could be found. However, this analysis failed to take into account the spectral wandering. In effect, spectra taken over a fixed time interval average the high-frequency data more than the low-frequency data. Data averaged over times inversely proportional to f showed no indication of a dependence of this fractional variance on f (see Fig. 6).

For a hierarchical picture, this dependence of the ensemble fractional variance of $S(f)$ on f is determined by how the average density of vertices on a branch changes with D, a more detailed feature than we wish to use initially to distinguish between generic pictures. However, a remarkable prediction emerges when we turn to the scaling properties of $S_2(f_2,f)$. The total fractional variance of $S(f)$ [i.e., the integral over f_2 of $S_2(f_2,f)$] will be inversely proportional to the density of vertices (per branch) at f, just as it would be inversely proportional to the droplet density. The frequency distribution (in f_2) of that variance depends on the distribution of rates for switching among branches. Thus the fraction of that variance that will be found in $S_2(f_2,f)$ in an octave around f_2 will be linearly proportional to the density of vertices at f_2. Therefore, the density of vertices drops out if we take the limit of the low-frequency part of $S_2(f_2,f)$ as f_2 approaches f (which does not require too much extrapolation). To a good approximation, $S_2(f_2,f)$ should depend only on f_2/f, not on the scale f, except for very large logarithmic differences between f_2 and f, regardless of whether the hierarchy itself is scale invariant.

What happens to the scaling of $S_2(f_2,f)$ for an interacting-droplet model? As with the hierarchical picture, the number density of the droplets will drop out to first order. However, the probability that two droplets will interact enough to show up in the time dependence

of the spectrum will depend on their size. Naturally, two large droplets are more likely to interact than two small ones. For droplet scaling to account for the broad range of relaxation times, $S_2(f_2,f)$ should be a decreasing function of f at constant f_2/f.

Thus we find a genuine difference between generalized droplet and hierarchical pictures. Physically, the essential point is that in a droplet picture the smaller droplets are affected by bigger droplets with a probability depending on their actual sizes. In a hierarchical picture, the smaller branches are systematically embedded in the bigger branches, independently of scale. Thus the droplet picture predicts scaling with a finite exponent, while the same exponent is zero for the hierarchical picture.

Taking a look at some real data in Figs. 6 and 7, we find $S_2(f_2,f)$ to be nearly scale invariant. Although the data in Fig. 7(b) deviate from scale invariance, the sign of the deviation is opposite to the prediction for interacting droplets.[4]

We have thus compared the dependences of $S_2(f_2,f)$ on f with the scale-invariant hierarchical prediction and with an interacting-droplet prediction in which the deviation from scale invariance is calculated from the difference in spectral exponents between the first and second spectra. The hierarchical fit is reasonable, but we just cannot fit the droplet picture. Therefore I shall give up trying to describe these data in terms of droplets.

V. IMPLICATIONS WITHIN A HIERARCHICAL FRAMEWORK

The illustrative pictures of either the Parisi or kinetic ultrametric trees idly drawn by theorists usually show mainly bifurcating vertices, with an occasional trifurcating vertex. While our experiments were under way, Israeloff would occasionally complain that he could not fit the white tail of the second spectra with a bifurcating tree. As he put it, something was wrong with the "foliation" of the tree. Naturally, I paid no attention to that kind of talk, since it scarcely seemed possible that we could even tell if there was a tree. However, he was right about fitting S_2. Furthermore, if the tree was bifurcating, where were the two-state random telegraph signals in $\delta R(t)$? β was small enough, particularly at low T, to afford repeated chances for most vertex events to occur before the next-higher vertex event. The detailed set of fluctuations available had a way of partially forgetting its initial value on a short time scale, before it was likely to be lost in transitions over higher vertices.

The only way we could explain this fast loss of memory was by postulating that each vertex in Fig. 2 usually should have more than two descending branches. Then usually on a given time scale $\delta R(t)$ would switch between enough states to make it hard to pick out two-state systems. This postulate, if true, would have a further implication. When an active vertex is temporarily lost or gained by transition over a higher vertex, the set of characteristic fluctuation rates lost or gained would not be a single delta function, but would contain several different rates—one less than the number of descendent branches. Although these rates would be comparable, since each would correspond to the same D, it would hardly be realistic to expect them all to be exactly equal. The low-frequency part of $S_2(f_2,f_a,f_b)$, produced by higher vertex events, should then be more correlated for bigger values of $|\ln(f_a/f_b)|$ than it would be if two-state systems with Lorentzian spectra were the units being gained or lost. So those strange cross second spectra, $S_2(f_2,f_a,f_b)$, that you thought I would not mention again have returned. As Fig. 8 shows, their low-frequency part extends to bigger values of $|\ln(f_a/f_b)|$ than it would in a bifurcating picture.

This argument, however, only pertains to the changes in $S(f)$ produced by losing or acquiring an active vertex by transitions over a higher vertex. If our picture is correct, the white part of the second spectrum comes from dynamics associated with a single vertex. Qualitatively, we guessed that these fluctuations in $S(f)$ should show less correlation between separated f's than would independent Lorentzians, since they correspond to swapping different characteristic times within the set provided by one vertex. The state cannot simultaneously be on a

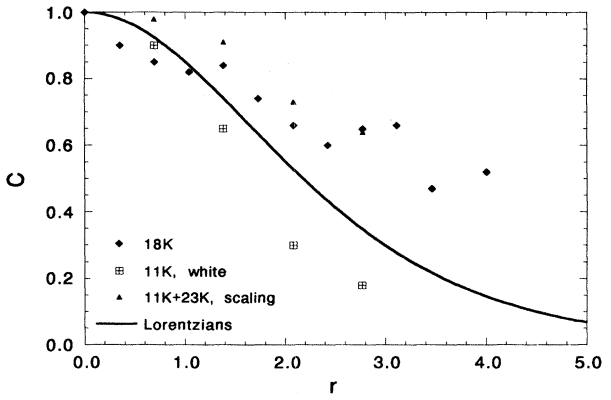

FIG. 8. Correlation coefficient C for fluctuations of the noise power at two frequencies, f_a and f_b, with $\ln(f_a/f_b)=r$. The solid curve, $r/\sinh(r)$, is predicted for independent Lorentzian contributions to S_1. The "18 K" points include mainly slow fluctuations in the noise power, and the "11K+23K, scaling" data include only slow fluctuations. The "11 K, white" data include only fast fluctuations.

[4]We have a guess as to why these data are further from the scaling prediction than the other two sets. The first two sets were taken while we were learning the ropes and involved sums of several sets of data taken with interruptions for He transfers, etc. The third set was taken with smoother experimental procedures and represented just one data set at fixed temperature. It is probably better to average over several cooldowns to approach an ensemble average, rather than sampling just one region of phase space, with inevitable random deviations from scaling.

faster equilibrating branch and a slower equilibrating branch, so there should be a negative correlation, as compared with our simplest case of independent Lorentzians. In fact, the white part of $S_2(f_2,f_a,f_b)$ does fall off more rapidly with $|\ln(f_a/f_b)|$ than it would if two-state systems with Lorentzian spectra were independently being gained or lost.

We argued before that in a hierarchical picture $S_2(f_2,f)$ does not depend on the density of vertices as f_2 approaches f. Does it then depend on anything? There are some small dependences on the tree topology, i.e., on the number of branches from each vertex. However, since that number is approximately measured, we then have a prediction for the absolute value of $S_2(f_2,f)$ for a hierarchy. The data do not fit that prediction; the magnitude of $S_2(f_2,f)$ falls short of expectations for a single hierarchy by a factor of 4 to 12. An *ad hoc* fit can be made simply by assuming that 4 to 12 hierarchies operate in parallel, averaging out all the non-Gaussian effects. This assumption, in retrospect, is highly reasonable, since our experimental samples are not cubes but rectangular solids, which become effectively two dimensional on scales of roughly 50 nm and one dimensional on scales of about 100 nm. Since the lower critical dimension of a spin glass is supposed to be between 2 and 3, loss of coherent behavior near the crossover length scale is not surprising.

The operational meaning of the coherence volume may not be entirely obvious. Within that coherence volume, the rearrangement of any group of spins changes the dynamical properties of all the smaller possible spin rearrangements. It is the independence of that volume on frequency that implies a systematic embedding of the faster modes within the slower modes.

In our experiments we measure properties of "states" that are long-lived collections of configurations, apparently related by a kinetic hierarchy. Using only this presumed hierarchical arrangement, we may determine some properties of $P(q)$, the probability density of finding two such states with overlap q. The probability density function for finding a vertex with more than one descendant with appreciable Boltzmann weight at some overlap q is, roughly speaking, $P(q)/y(q)$, where $y(q) = \int_q^1 P(q')dq'$.

Since the parameter β in the second spectrum depends linearly on the density of vertices in log-time (or log-frequency) space, it provides a measure of $P(q)/y(q)$, so long as one knows $dq/d\ln(f)$ approximately. This derivative, i.e., the typical loss of overlap versus log time, is given by the fluctuation-dissipation theorem and by $\chi''(f)$, as long as one assumes a mean-square change of magnetization linear in D. Thus we can put together the measured values of β with known values of χ'' to obtain values for $P(q)/y(q)$ at several different values of q and T. However, since the particular frequency window of the experiments is strongly constrained, we cannot independently vary q much at fixed T. We found in two samples $P(q)/y(q) \approx 35$ for $0.4T_G < T < 0.8T_G$.

If the pure states of the Parisi theory map in a simple fashion onto the metastable states of the mesoscopic system, a comparison of our measured $P(q)/y(q)$ with the prediction of the Parisi theory would be in order. Our result is more than an order of magnitude larger than expected from mean-field theory (Young, 1983). However, at least one theoretical work had predicted that in finite dimensions the extent of replica symmetry breaking [and hence $P(q)/y(q)$] would be greater than in mean-field theory (Georges *et al.*, 1990).

Our results should not by any means be taken to imply that droplet approaches should be abandoned as theorists turn their attention to calculating loop corrections to the mean-field theory. In fact, as the standard closing cliché goes, our results raise as many questions as they answer.

If the hierarchical interpretation of our results makes sense, are the parameters, such as the coherence volume and the vertex density, consistent with values needed to interpret nonlinear macroscopic measurements? Can the finite-size-effect measurements also be interpreted in some not too drastically modified hierarchical picture? Can the set of spin-spin correlations appearing in the universal conductance fluctuations (UCF's) be well enough elucidated to provide another handle on the lack of compactness of the coherent droplets, or on the distances over which these correlations are scrambled on thermal cycling? Under what circumstances do the spin-dependent UCF's survive unchanged under cycling to large fields, as found by de Vegvar *et al.* (1991) but not by us? Why are no effects of thermal chaos found in the UCF's? (Alers *et al.*, 1992). We have addressed some of these questions elsewhere, but only tentatively.

Our measurements were made on a single material within a moderately large temperature regime. What happens at lower temperatures? What would happen at longer times, if anybody figured out how to do the measurements? Do materials, especially insulators, with only short-range interactions show similar effects? Are the incipient SDW's in Cu important in creating an unusually long-range interaction? What role does the unusually weak anisotropy of *Cu*Mn play in determining the mesoscopic behavior? Answering these questions will require more experiments.

ACKNOWLEDGMENTS

This work was supported primarily by NSF DMR 89-20538 through the Materials Research Laboratory and also by NSF DMR 89-22967.

REFERENCES

Alers, G. B., M. B. Weissman, and N. E. Israeloff, 1992, Phys. Rev. B **46**, 507.

Al'tshuler, B. L., and B. Z. Spivak, 1985, Pis'ma Zh. Eksp. Teor. Fiz. **42**, 363 [JETP Lett. **42**, 447 (1985)].

Bachas, C., and B. A. Huberman, 1986, Phys. Rev. Lett. **57**,

1965, 2877.
Binder, K., and A. P. Young, 1986, Rev. Mod. Phys. **58**, 801.
Bray, A. J., and M. A. Moore, 1987, Phys. Rev. Lett. **58**, 57.
de Vegvar, P. G. N., L. P. Lévy, and T. A. Fulton, 1991, Phys. Rev. Lett. **66**, 2380.
Dotsenko, V. S., M. V. Feigel'man, and L. B. Ioffe, 1990, *Spin Glasses and Related Phenomena* (Harwood, Glasgow, U.K.) [Sov. Sci. Rev. A Phys. **15**, Part 1].
Feigel'man, M. V., and L. B. Ioffe, 1984, J. Phys. (Paris) Lett. **45**, L-475.
Feng, S., A. J. Bray, P. A. Lee, and M. A. Moore, 1987, Phys. Rev. B **36**, 5624.
Fischer, K. H., and J. A. Hertz, 1991, *Spin Glasses* (Cambridge University, Cambridge, England).
Fisher, D. S., and D. A. Huse, 1988a, Phys. Rev. B **38**, 373.
Fisher, D. S., and D. A. Huse, 1988b, Phys. Rev. B **38**, 386.
Garfunkel, G. A., and M. B. Weissman, 1990, J. Vac. Sci. Tech. B **8**, 1087.
Gavrin, A., J. R. Childress, C. L. Chien, B. Martinez, and M. B. Salamon, 1990, Phys. Rev. Lett. **64**, 2438.
Georges, A., M. Mezard, and J. S. Yedida, 1990, Phys. Rev. Lett. **64**, 2937.
Ioffe, L. B., and M. V. Feigel'man, 1985, Zh. Eksp. Teor. Fiz. **88**, 604 [Sov. Phys. JETP **61**, 354 (1985)].
Israeloff, N. E., G. B. Alers, and M. B. Weissman, 1991, Phys. Rev. B **44**, 12613.
Israeloff, N. E., M. B. Weissman, G. J. Nieuwenhuys, and J. Kosiorowska, 1989, Phys. Rev. Lett. **63**, 794.
Lederman, M., R. Orbach, J. Hammann, and M. Ocio, 1991, Phys. Rev. B **44**, 7403.
Maritan, A., and A. L. Stella, 1986, J. Phys. A **19**, L269.
Meiss, J., and E. Ott, 1986, Phys. Rev. Lett. **55**, 2741.
Mézard, M., G. Parisi, and M. A. Virasoro, 1987, Eds., *Spin Glass Theory and Beyond* (World Scientific, Singapore).
Mulder, C. A. M., A. J. van Duyneveldt, and J. A. Mydosh, 1981, Phys. Rev. B **23**, 1384.
Mydosh, J. A., 1988, J. Appl. Phys. **63**, 5415.
Ocio, M., H. Bouchiat, and P. Monod, 1986, J. Magn. Magn. Mater. **54-57**, 11.
Ogielski, A. T., and D. L. Stein, 1985, Phys. Rev. Lett. **55**, 1634.
Overhauser, A. W., 1959, Phys. Rev. Lett. **3**, 414.
Paladin, G., M. Mézard, and C. De Dominicis, 1985, J. Phys. (Paris) Lett. **46**, L985.
Rammal, R., G. Toulouse, and M. A. Virasoro, 1986, Rev. Mod. Phys. **58**, 765.
Reim, W., R. H. Koch, A. P. Malozemoff, M. B. Ketchen, and H. Maletta, 1986, Phys. Rev. Lett. **57**, 905.
Sandlund, L., P. Granberg, L. Lundgren, P. Norblad, P. Svedlindh, J. A. Cowen, and G. G. Kenning, 1989, Phys. Rev. B **40**, 869.
Schreckenberg, M., 1985, Z. Phys. B **60**, 483.
Sherrington, D., and S. Kirkpatrick, 1975, Phys. Rev. Lett. **35**, 1792.
Sibani, P., 1987, Phys. Rev. B **35**, 8572.
Sompolinsky, H., and A. Zippelius, 1982, Phys. Rev. B **25**, 6860.
Weissman, M. B., 1988, Rev. Mod. Phys. **60**, 537.
Weissman, M. B., N. E. Israeloff, and G. B. Alers, 1992, J. Magn. Magn. Mater. **114**, 87.
Werner, S. A., 1990, Comments Condens. Matter Phys. **15**, 55.
Young, A. P., 1983, Phys. Rev. Lett. **51**, 1206.